Sensor Fault Diagnosis in Quadrotors Using Nonlinear Adaptive Estimators

Remus C Avram[1], Xiaodong Zhang[2] and Jacob Campbell[3]

[1,2] *Wright State University, Dayton, Ohio, 45404, USA*
avram.3@wright.edu
xioadong.zhang@wright.edu

[3] *Air Force Research Laboratory, Dayton, OH, 45404, USA*
jacob.campbell.3@us.af.mil

ABSTRACT

Unmanned Aerial Vehicles (UAVs) have attracted significant attentions in recent years due to their potentials in various military and civilian applications. Small UAVs are often equipped with low-cost and lightweight micro-electro-mechanical systems (MEMS) inertial measurement units including 3-axis gyro, accelerometer and magnetometer. The measurements provided by gyros and accelerometers often suffer from bias and excessive noise as a result of temperature variations, vibration, etc. This paper presents a sensor fault diagnostic method for quadrotor UAVs. Specifically, we consider the faults in the gyro and accelerometer. A model-based sensor fault detection and isolation (FDI) estimation method is presented. The proposed FDI method adopts the idea that accelerometer and gyroscopic measurements coincide with the translational and rotational forces represented in the UAV dynamics. Thus, the faults in accelerometer and gyroscope can be represented as virtual actuator faults in the quadrotor state equations. Two diagnostic estimators are designed to provide structured FDI residuals allowing simultaneous detection and isolation of gyroscope and accelerometer sensor bias. In addition, nonlinear adaptive estimators are designed to provide an estimate of the unknown sensor bias. The parameter convergence property of the adaptive estimation scheme is analyzed. Simulation studies utilizing a nonlinear quadrotor UAV model are used to illustrate the effectiveness of the proposed method.

1. INTRODUCTION

Unmanned Aerial Vehicles (UAVs) have attracted significant attentions in recent years due to their potentials in various military and civilian applications, including security patrol, search and rescue in hazardous environment, surveillance and classification, attack and rendezvous (Shima & Rasmussen, 2008). In addition, compared with manned systems, the reductions in operations and support costs for unmanned vehicles offer the advantage for life cycle cost savings (US Dept. of Defense, 2012). The potential capabilities offered by unmanned vehicles have been well recognized and continue to expand. In manned systems, the human operator functions as the central integrator of the onboard systems to achieve their operational capabilities. Due to the requirement of autonomous operations without a human operator, autonomous control of UAVs is much more challenging. For instance, UAVs currently suffer mishaps at 10 to 100 times the rate incurred by their manned counterparts (US Dept. of Defense, 2012, 2000). In order to enhance the reliability, survivability and autonomy of UAVs, advanced intelligent control and health management technologies are required, which will enable UAVs to have the capabilities of state awareness and self-adaptation (Sharifi, Mirzaei, Gordon, & Zhang, 2010; Vachtsevanos, Tang, Drozeski, & Gutierrez, 2005).

Most quadrotors used in research, are often equipped with low-cost and lightweight micro-electro-mechanical systems (MEMS) inertial measurement units (IMU) including 3-axis gyro, accelerometer and magnetometer. These sensors serve an essential role in most quadrotor control schemes. However, due to their intrinsic components and fabrication process, IMUs are vulnerable to exogenous signals and prone to faults. Specifically, accelerometer and gyroscope measurements are susceptible to bias and excessive noise as a result of temperature variation, vibration, etc. The detection and estimation of accelerometer and gyroscope faults plays a crucial role in the safe operations of quadrotors.

Several researchers have investigated the problem of quadrotor IMU sensor fault diagnosis based on linearized quadrotor dynamic model (Sharifi et al., 2010; Freddi, Longhi, & Monteriú, 2009; Dydek, Annaswamy, & Lavretsky, 2013; Here-

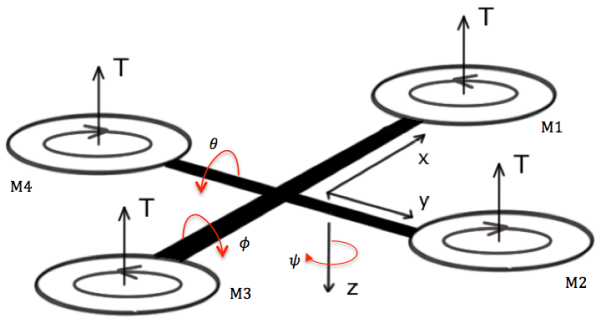

Figure 1. Quadrotor Model in "+" configuration.

dia, Ollero, Mahtani, & Bejar, 2005). A few papers have considered the Luenberger or Kalman filter based observers in order to generate residuals for fault diagnosis purposes (see, for example (Freddi et al., 2009; Heredia et al., 2005; Lantos & Marton, 2011)). These methods rely on linearization of the system around a set of equilibrium points. However, the dynamics of the quadrotor are highly nonlinear and the states can be strongly coupled. In recent years, considerable research effort has been devoted to fault diagnosis of nonlinear systems under various kinds of assumptions and fault scenarios (Blanke, Kinnaert, Lunze, & Staroswiecki, 2005). In this paper we present a nonlinear method for detecting, isolating and estimating sensor bias faults in accelerometer and gyroscope measurements of quadrotor UAVs. Based on the fact that the accelerometer and the gyroscope measure forces/torque acting directly on the UAV body, the quadrotor dynamics are expressed in terms of the IMU sensor measurements. Two diagnostic estimators are designed to provide structured fault detection and isolation (FDI) residuals allowing simultaneous detection and isolation of gyroscope and accelerometer sensor bias. In addition, by utilizing nonlinear adaptive estimation techniques (Zhang, Polycarpou, & Parsini, 2001), adaptive estimators are employed to provide an estimate of the unknown sensor bias. The parameter convergence property of the adaptive estimation scheme is analyzed.

The remainder of the paper is organized as follows. Section II formulates the problem of sensor FDI for quadrotor UAVs. The proposed fault detection and isolation method is presented in Section III. Section IV describes the adaptive estimator algorithms for estimation of sensor bias magnitude and provides conditions for parameter convergence. Section V and VI present simulation results and direction of future research, respectively.

2. PROBLEM FORMULATION

Several works focus on quadrotor modeling see for example (Bramwell, Done, & Balmford, 2001) and (Castillo, Lozano, & Dzul, 2005). More recently, (Pounds, Mahony, & Gresham, 2004; Bangura & Mahony, 2012) have aimed for higher modeling accuracy by including drag force, Coriolis effects, blade flapping effects etc. Accurate modeling plays an important role in quadrotor control, especially in the case of aggressive maneuvers, tight group formations, etc. However, when the quadrotor is in a non-aggressive maneuver state, these effects become very small in comparison to gravitational pull and thrust generated by the rotors. As in (Leishman, Jr., Beard, & McLain, 2014) and (Martin & Salaün, 2010), the dynamic model used in this paper considers the gravity, thrust generated by the rotors and drag forces acting on the quadrotor body. Figure 1 shows a simplifed model of the quadrotor along with the assumed body frame orientation and Euler angles convention using the right-hand rule. The quadrotor nominal system dynamics are derived from the Newton-Euler equations of motion and are given by:

$$\dot{p}_E = v_E \tag{1}$$

$$\dot{v}_E = \frac{1}{m} R_{EB}(\eta) \left(\begin{bmatrix} 0 \\ 0 \\ -T \end{bmatrix} - c_{\mathbf{d}} v_B \right) + \begin{bmatrix} 0 \\ 0 \\ g \end{bmatrix} \tag{2}$$

$$\dot{\eta} = \begin{bmatrix} 1 & \sin\phi\tan\theta & \cos\phi\tan\theta \\ 0 & \cos\phi & -\sin\phi \\ 0 & \sin\phi\sec\theta & \cos\phi\sec\theta \end{bmatrix} \omega \tag{3}$$

$$\begin{bmatrix} \dot{p} \\ \dot{q} \\ \dot{r} \end{bmatrix} = \begin{bmatrix} \frac{J_y - J_z}{J_x} qr \\ \frac{J_z - J_x}{J_y} pr \\ \frac{J_x - J_y}{J_z} pq \end{bmatrix} + \begin{bmatrix} \frac{1}{J_x}\tau_\phi \\ \frac{1}{J_y}\tau_\theta \\ \frac{1}{J_z}\tau_\psi \end{bmatrix} \tag{4}$$

where $p_E \in \mathbb{R}^3$ is the inertial position, $v_E \in \mathbb{R}^3$ is the velocity expressed in the Earth frame, $\eta = [\phi, \theta, \psi]^T \in \mathbb{R}^3$ are the roll, pitch and yaw Euler angles, respectively, and $\omega = [p\, q\, r]^T$ represents the angular rates, m is the mass of the quadrotor, and g is the gravitational acceleration. The terms J_x, J_y and J_z represent the quadrotor inertias about the body x-, y- and z-axis, respectively. Note that the quadrotor is assumed to be symmetric about the xz and yz planes (i.e. the product of inertias is zero). T represents the total thrust generated by the rotors, τ_ϕ, τ_θ, τ_ψ are the torques acting on the quadrotor around the body x-, y- and z-axis, respectively. The term $c_{\mathbf{d}} v_B$ represents the drag force acting on the vehicle frame, with $c_{\mathbf{d}}$ being drag force coefficient and v_B is the velocity of the UAV relative to the body frame.

The system model described by Eq (1) - (4) is expressed with the velocity relative to the inertial frame. The inertial coordinate system is assumed to have the positive x-axis pointing North, the positive y-axis pointing East and positive z-axis pointing down towards the Earth's center. The transformation from the body frame to inertial frame is given by the rotation matrix R_{EB} and is defined based on a 3-2-1 rotation sequence as follows:

$$R_{EB}(\eta) = \begin{bmatrix} c\theta c\psi & s\phi s\theta c\psi - c\phi s\psi & c\phi s\theta c\psi + s\phi s\psi \\ c\theta s\psi & s\phi s\theta s\psi + c\phi c\psi & c\phi s\theta s\psi - s\phi c\psi \\ -s\theta & s\phi c\theta & c\phi c\theta \end{bmatrix}$$

where $s\cdot$ and $c\cdot$ are short hand notations for the $\sin(\cdot)$ and $\cos(\cdot)$ functions, respectively.

MEMS sensors, such as accelerometers and gyroscopes, measure forces and moments acting in the body frame. The quantity expressed inside the parenthesis in the inertial velocity Eq. (2), represents all the forces acting on the body. Therefore, the velocity dynamic equation can be adjusted to reflect accelerometer measurements. Similarly, the evolution of Euler angles can be rewritten in terms of gyroscope measurements (Leishman et al., 2014; Ireland & Anderson, 2012). By considering IMU measurement susceptibility to a constant bias drift, the accelerometer and gyroscope sensor measurements are given by:

$$y_a = a + b_a = \frac{1}{m}\left(\begin{bmatrix} 0 \\ 0 \\ -T \end{bmatrix} - c_{\mathbf{d}} v_B\right) + b_a \tag{5}$$

$$y_\omega = \omega + b_\omega = \begin{bmatrix} p \\ q \\ r \end{bmatrix} + b_\omega \tag{6}$$

where $y_a \in \mathbb{R}^3$ and $y_\omega \in \mathbb{R}^3$ are the measured accelerometer and gyro quantities, respectively, $b_a \in \mathbb{R}^3$ and $b_\omega \in \mathbb{R}^3$ are the possible constant bias in accelerometer and gyroscope measurements, respectively, and a represents the nominal acceleration measurement without bias, that is:

$$a = \frac{1}{m}\left(\begin{bmatrix} 0 \\ 0 \\ -T \end{bmatrix} - c_{\mathbf{d}} v_B\right) \tag{7}$$

In addition, as in (Ireland & Anderson, 2012) and (Lantos & Marton, 2011), it is assumed that the position measurements in the Earth frame and Euler angles measurements are available. For instance, these measurements can be generated by a camera-based motion capture system, a technology commonly employed for in-door UAV flight (Guenard, Hamel, & Mahony, 2008). Hence, the system model can be augmented by the following output equations:

$$y_p = p_E \tag{8}$$

$$y_\eta = \eta \tag{9}$$

The objective of this research focuses on the detection, isolation and estimation of sensor bias in accelerometer and gyroscope measurements.

3. FAULT DETECTION AND ISOLATION

This section presents the proposed method for detecting and isolating sensor faults in accelerometer and gyroscope measurements. Substituting the sensor model from Eq (5)-(6) into the systems dynamics Eq (1)-(4), we obtain:

$$\dot{p}_E = v_E \tag{10}$$

$$\dot{v}_E = R_{EB}(\eta) y_a + \begin{bmatrix} 0 \\ 0 \\ g \end{bmatrix} - R_{EB}(\eta) b_a \tag{11}$$

$$\dot{\eta} = T(\eta) y_\omega - T(\eta) b_\omega \tag{12}$$

$$\begin{bmatrix} \dot{p} \\ \dot{q} \\ \dot{r} \end{bmatrix} = \begin{bmatrix} \frac{J_y - J_z}{J_x} qr \\ \frac{J_z - J_x}{J_y} pr \\ \frac{J_x - J_y}{J_z} pq \end{bmatrix} + \begin{bmatrix} \frac{1}{J_x}\tau_\phi \\ \frac{1}{J_y}\tau_\theta \\ \frac{1}{J_z}\tau_\psi \end{bmatrix} \tag{13}$$

where $T(\eta)$ is the rotation matrix relating angular rates to Euler angle rates and is given by:

$$T(\eta) = \begin{bmatrix} 1 & \sin\phi\tan\theta & \cos\phi\tan\theta \\ 0 & \cos\phi & -\sin\phi \\ 0 & \sin\phi\sec\theta & \cos\phi\sec\theta \end{bmatrix}.$$

In order to eliminate the coupling between translational velocity and angular rates when the quadrotor dynamics are represented with velocity relative to the body frame, the quadrotor dynamics are expressed with velocity relative to the earth frame. As can be seen from Eq (10)-(13), a bias in accelerometer measurements affects only the position and velocity states. Conversely, gyroscope measurements affect only Euler angles and angular rates states. Based on this observation, it follows naturally to also divide the fault diagnosis of these two sensor faults. The proposed fault detection, isolation and estimation architecture is shown in Figure 2. As can be seen, two FDI estimators monitor the system for fault occurrences in accelerometer and gyroscope measurements. Once a fault is detected and isolated, the corresponding nonlinear adaptive estimator is activated for sensor bias estimation purposes.

3.1. Gyroscope Bias Diagnostic Estimator

As can be seen from the dynamics of the quadrotor, given by equations (10)-(13), the bias in the gyroscope measurements only affects the attitude and rotation dynamics given by Eq (12)-(13). Since the attitude angles given by the state vector η are assumed to be measurable (see Section 2), based on Eq (12)-(13) and adaptive estimation schemes, such as the series-parallel model (Ioannou & Sun, 1996), the fault diagnostic estimator for the gyroscope bias can be designed as follows:

$$\dot{\hat{\eta}} = -\Lambda(\hat{\eta} - \eta) + T(\eta) y_\omega \tag{14}$$

where $\hat{\eta} \in \mathbb{R}^3$ are the Euler angle estimates, $\Lambda \in \mathbb{R}^{3\times3}$ and $\Gamma \in \mathbb{R}^{3\times3}$ are positive-definite, diagonal design matrices. Let the Euler angle estimation error be defined as:

$$\tilde{\eta} \triangleq \eta - \hat{\eta} \tag{15}$$

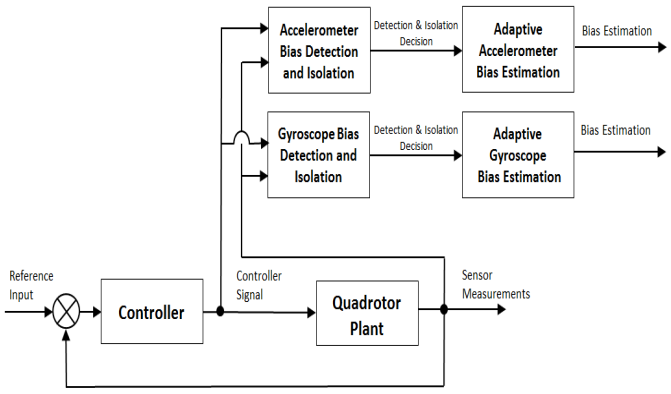

Figure 2. Fault Detection, Isolation and Estimation Architecture.

Then, based on Eq (12) and Eq (14), we have:

$$\dot{\tilde{\eta}} = \dot{\eta} - \dot{\hat{\eta}} = -\Lambda\tilde{\eta} - T(\eta)b_\omega \tag{16}$$

Equation (16) guarantees that the Euler angles estimation error converges asymptotically to zero in the absence of gyroscope sensor bias. In addition, in the presence of a non-zero bias b_ω, based on Eq (16) it can be seen that the residual $\tilde{\eta}$ will deviate from zero. Therefore, if any component of the state estimation error $\tilde{\eta}$ is significantly different from zero, we can conclude that a fault in the gyroscope measurements has occurred.

3.2. Accelerometer Bias Diagnostic Estimator

The dynamics of UAV position and velocity relative to the inertial frame given by Eq (10) and Eq (11) can be put in the following state space model:

$$\begin{aligned} \dot{x} &= Ax + f(\eta, y_a) + G_a(\eta)b_a \\ y &= Cx \end{aligned} \tag{17}$$

where $x = [p_E^T \; v_E^T]^T$, $y = p_E$, and

$$A = \begin{bmatrix} 0_{3\times3} & I_3 \\ 0_{3\times3} & 0_{3\times3} \end{bmatrix},$$

$$G_a(\eta) = \begin{bmatrix} 0_{3\times3} \\ -R_{EB} \end{bmatrix},$$

$$f(\eta, y_a) = \begin{bmatrix} 0_{3\times1} \\ R_{EB}y_a + \begin{bmatrix} 0 \\ 0 \\ g \end{bmatrix} \end{bmatrix}$$

and $C = [I_3, \; 0_{3\times3}]$, where I_3 is a 3×3 identity matrix, $0_{3\times3}$ is a 3×3 matrix with all entries zero and $0_{3\times1}$ is a 3×1 zero vector. Based on this configuration, the following fault diagnostic observer is chosen :

$$\begin{aligned} \dot{\hat{x}} &= A\hat{x} + f(\eta, y_a) + L(y - \hat{y}) \\ \hat{y} &= C\hat{x} \end{aligned} \tag{18}$$

where $\hat{x} \in \mathbb{R}^6$ represents the inertial position and velocity estimation, $\hat{y} \in \mathbb{R}^3$ are the predicted position outputs, and L is a design matrix chosen such that the matrix $\bar{A} \triangleq (A - LC)$ is stable. From the definition of matrices A and C given by Eq (17) it is straightforward to show that the system is observable. Therfore, the matrix L can be easily designed. Defining the state estimation error as: $\tilde{x} \triangleq x - \hat{x}$ and the quadrotor position estimation error as $\tilde{y} \triangleq y - \hat{y}$, it follows that:

$$\begin{aligned} \dot{\tilde{x}} &= \bar{A}\tilde{x} + G_a(\eta)b_a \\ \tilde{y} &= C\tilde{x} \; . \end{aligned} \tag{19}$$

Clearly, the output estimation error $\tilde{y}$ reaches zero asymptotically in the absence of the accelerometer bias b_a. Furthermore it can be seen from Eq (19) the residual $\tilde{y}$ is only sensitive to the bias b_a. Therefore, if any component of the position estimation error $\tilde{y}$ deviates significantly from zero, we can conclude that a fault in the accelerometer sensor measurement has occurred.

3.3. Fault Detection and Isolation Decision Scheme

As described in section 3.1 and 3.2, the two fault diagnostic estimators are designed such that each of them is only sensitive to one type of sensor faults. Based on this observation, the residuals $\tilde{\eta}$ and $\tilde{y}$ generated by Eq (16) and Eq (19) can also be used as structured residuals for fault isolation. More specifically, we have the following fault detection and isolation decision scheme:

- In the absence of any faults, all components of the residuals $\tilde{\eta}$ and $\tilde{y}$ should be close to zero.
- If all components of the residual $\tilde{\eta}$ remain around zero, and at least one component of the residual $\tilde{y}$ is significantly different from zero, then we conclude that an accelerometer fault has occurred.
- If all components of the residual $\tilde{y}$ remain around zero, and at least one component of the residual $\tilde{\eta}$ is significantly different from zero, then we conclude that a gyroscope fault has occurred.
- If at least one component of the residual $\tilde{\eta}$ is significantly different from zero, and at least one component of the residuals $\tilde{y}$ is significantly different from zero, then we conclude that both a gyroscope and accelerometer sensor measurement fault has occurred.

The above FDI decision scheme is summarized in Table 1, where "0" represents nearly zero residuals, and "1" represents significantly large residuals.

Table 1. Fault Isolation Decision Truth Table.

	No Fault	Gyro Bias	Accel Bias	Accel & Gyro Bias
$\tilde{\eta}$	0	0	1	1
$\tilde{y}$	0	1	0	1

4. FAULT ESTIMATION

After a sensor fault is detected and isolated, it is also crucial to provide an estimation of the sensor bias to improve the performance of the closed loop control system. As shown in Figure 2, once a fault has been detected and isolated, the corresponding nonlinear adaptive bias estimator is activated with the purpose of estimating the fault magnitude in the accelerometer and/or gyroscope measurements. In this section, we describe the design of nonlinear adaptive estimators for sensor bias estimation.

4.1. Accelerometer Fault Estimation

Based on Eq (17), the adaptive observer for estimating the accelerometer bias magnitude is chosen as:

$$\dot{\hat{x}} = A\hat{x} + f(\eta, y_a) + L(y - \hat{y}) + G_a(\eta)\hat{b}_a + \Omega\dot{\hat{b}}_a \quad (20)$$

$$\dot{\Omega} = (A - LC)\Omega + G_a(\eta) \quad (21)$$

$$\hat{y} = C\hat{x} \quad (22)$$

where $\hat{x}$ is the estimated position and velocity vector, $\hat{y}$ is the estimated position output, $\hat{b}_a$ is the estimated sensor bias, and L is the observer gain matrix. The adaptation in the above adaptive estimator arises due to the unknown bias b_a. The adaptive law for updating $\hat{b}_a$ is derived using Lyapunov synthesis approach (Ioannou & Sun, 1996; Zhang, 2011). Specifically, the adaptive algorithm is given by:

$$\dot{\hat{b}}_a = \Gamma\Omega^T C^T \tilde{y}_a \quad (23)$$

where $\Gamma > 0$ is a symmetric and positive-definite learning rate matrix, and $\tilde{y}_a \triangleq y_a - \hat{y}_a$ is the output estimation error. Let us also define the state estimation error $\tilde{x} \triangleq x - \hat{x}$. Then, based on Eq (17) and Eq (20), the dynamics governing the state estimation error are given by:

$$\dot{\tilde{x}} = \bar{A}\tilde{x} - G_a(\phi, \theta, \psi)\tilde{b}_a - \Omega\dot{\tilde{b}}_a \quad (24)$$

where $\bar{A} \triangleq A - LC$ and $\tilde{b}_a \triangleq \hat{b}_a - b_a$ is the parameter estimation error. By substituting $G_a(\eta) = \dot{\Omega} - (A - LC)\Omega$ (see Eq (21)) into Eq (24), we have

$$\begin{aligned} \dot{\tilde{x}} &= \bar{A}\tilde{x} - (\dot{\Omega} - \bar{A}\Omega)\tilde{b}_a - \Omega\dot{\tilde{b}}_a \\ &= \bar{A}(\tilde{x} + \Omega\tilde{b}_a) - \dot{\Omega}\tilde{b}_a - \Omega\dot{\tilde{b}}_a \ . \end{aligned} \quad (25)$$

By defining $\bar{x} \triangleq \tilde{x} + \Omega\tilde{b}_a$, the above equation can be rewritten as

$$\dot{\bar{x}} = \bar{A}\bar{x} \ . \quad (26)$$

In addition, the adaptive parameter estimation algorithm (see Eq (23)) can be rewritten as:

$$\begin{aligned} \dot{\hat{b}}_a &= \Gamma\Omega^T C^T \tilde{y}_a \\ &= \Gamma\Omega^T C^T C\tilde{x} \\ &= \Gamma\Omega^T C^T C(\bar{x} - \Omega\tilde{b}_a). \end{aligned} \quad (27)$$

Because the bias b_a is constant, we have $\dot{\tilde{b}}_a = \dot{\hat{b}}_a$. Thus, Eq (27) can be rewritten as:

$$\dot{\tilde{b}}_a = \Gamma\Omega^T C^T C\bar{x} - \Gamma\Omega^T C^T C\Omega\tilde{b}_a. \quad (28)$$

Based on Eq (26), we know $\bar{x}$ converges asymptotically to zero, since $\bar{A}$ is stable by design. In addition, if there exists constants $\alpha_0 > 0$, $T_0 > 0$ and α_1 such that the following condition is satisfied:

$$\alpha_1 I \geq \frac{1}{T_0}\int_t^{t+T_0} \Omega^T C^T C\Omega d\tau \geq \alpha_0 I \quad (29)$$

then we can conclude that the $\tilde{b}_a$ will converge to zero, that is $\hat{b}_a$ converges to the actual value b_a. It is worth noting that the condition given by Eq (29) provides the required persistence of excitation for parameter convergence (Ioannou & Sun, 1996). The nature of UAV flight provides vibrations in practical applications, which may lead to adequate levels of excitation. In addition, this condition can be satisfied by commanding the UAV to perform certain maneuvers.

4.2. Gyroscope Fault Estimation

Based on Eq (12), after the presence of a gyroscope bias fault is detected, the following adaptive estimator is activated in order to estimate the bias in the gyroscope sensor:

$$\dot{\hat{\eta}} = -\Lambda(\hat{\eta} - \eta) + T(\eta)y_\omega - T(\eta)\hat{b}_\omega \quad (30)$$

$$\dot{\hat{b}}_\omega = \Gamma T(\eta)(\eta - \hat{\eta}) \quad (31)$$

where $\hat{\eta}$ is the Euler angle estimate, $\hat{b}_\omega$ represents the estimation of the sensor bias, Λ and Γ are positive definite design matrices. The adaptive law for estimating the bias in gyroscope measurements in Eq (31) is derived using Lyapunov synthesis approach (Ioannou & Sun, 1996). The adaptive scheme in Eq. (30) ensures that the attitude angle estimation error $\tilde{\eta} \triangleq \eta - \hat{\eta}$ converges asymptotically to zero. In addition, in order to ensure parameter convergence, $T(\eta)$ will also have to satisfy the persistence of excitation condition (Ioannou & Sun, 1996), that is:

$$\alpha_1 I \geq \frac{1}{T_0}\int_t^{t+T_0} T(\eta)^T T(\eta) d\tau \geq \alpha_0 I \quad (32)$$

for some constants $\alpha_1 \geq \alpha_0 > 0$ and $T_0 > 0$ and for all $t \geq 0$. Again, we note that vibration present in UAV flight may offer adequate excitation. Additionally, the UAV can be commanded to perform certain maneuvers in order to reach the required levels of persistence of excitation.

5. SIMULATION RESULTS

In this section, we present some simulation results in order to illustrate the effectiveness of the proposed sensor bias diagnosis method. Specifically, two cases are studied while the quadrotor is commanded to move along a circular trajectory with a radius of 4 meters for a period of 20 seconds. We control the position and yaw rate of the quadrotor by means of state feedback using a linear quadratic regulator. As previously shown, the fault diagnosis technique employed in this approach is independent of the structure of the controller. Therefore, for brevity, the discussion on the control design is purposely omitted.

The first case studied corresponds to a bias drift in accelerometer measurements. Specifically, at time $t = 10s$ we injected a constant bias of $b_a = [0.2,\ 0.1,\ 0.5]^T m/s^2$ in the accelerometer measurements. Figure 3 shows the FDI residuals generated by the two diagnostic estimators described by Eq (14) and Eq (18), respectively. As can be seen, the components of the residual generated by the estimator corresponding to the accelerometer bias fault become nonzero shortly after fault occurrence, while all residual components generated by the gyroscope fault diagnostic estimator remain zero. Based on the detection and isolation logic given in Table 1, we can conclude that a fault has occurred in the accelerometer measurement. In addition, Figure 4 shows the estimation of the bias in the accelerometer for each axis, respectively, provided by the adaptive estimator (see Eq (23)). As can be seen, the bias estimate correctly reaches the actual bias values in the accelerometer measurements.

The second case corresponds to a bias in the gyroscope measurements injected at time $t = 10s$. The bias magnitude considered is given by $b_\omega = [10°,\ 5°,\ 1°]^T$. Figure 5 shows the time behaviors of the residuals generated by the two diagnositc estimators. As can be seen, the FDI residuals generated by the diagnostic estimator corresponding to the gyroscope fault become nonzero shortly after fault occurrence, and the residuals generated by the estimate corresponding to accelerometer fault always remain zero. Therefore, based on the detection and isolation decision logic given in Table 1, we can conclude that a fault has occurred in gyroscope measurements. Figure 6 shows the estimate of the bias in gyroscope roll, pitch and yaw measurements. As it can be seen, the bias estimate reaches the actual values of the bias in the sensor.

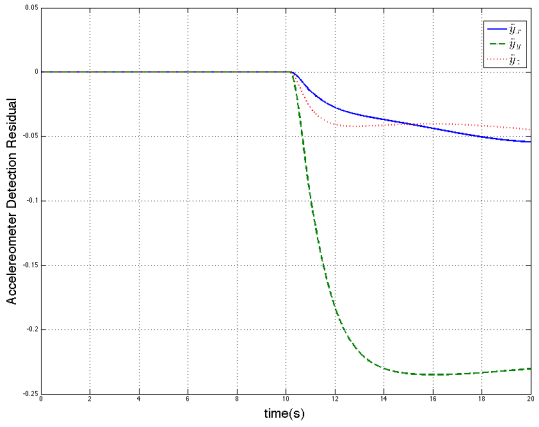

(a) Residuals generated by the diagnostic estimator corresponding to accelerometer bias

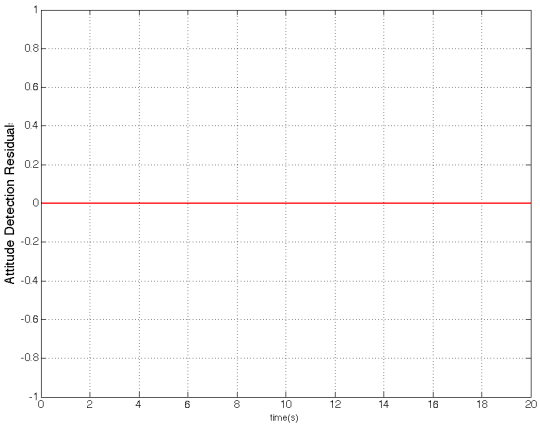

(b) Residuals generated by the diagnostic estimator corresponding to gyroscope bias

Figure 3. Fault detection and isolation of accelerometer bias.

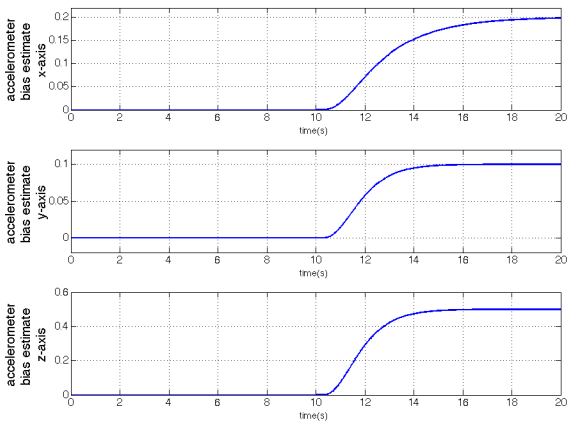

Figure 4. Estimation of accelerometer bias

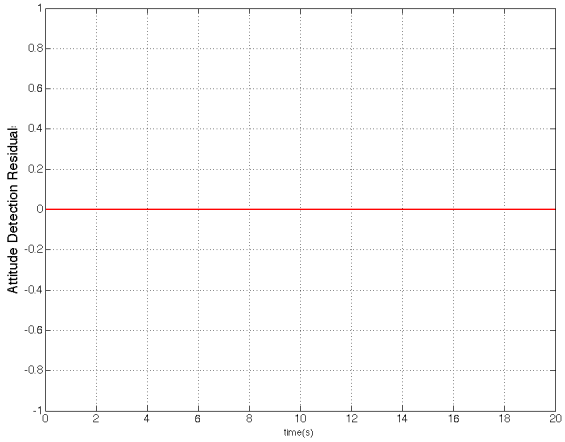

(a) Residuals generated by the diagnostic estimator corresponding to accelerometer bias

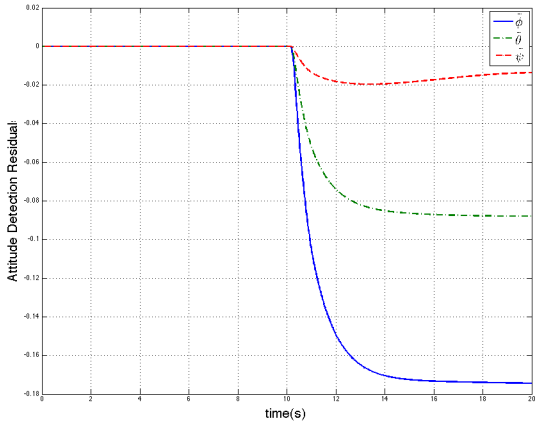

(b) Residuals generated by the diagnostic estimator corresponding to accelerometer bias

Figure 5. Fault detection and isolation of gyroscope bias.

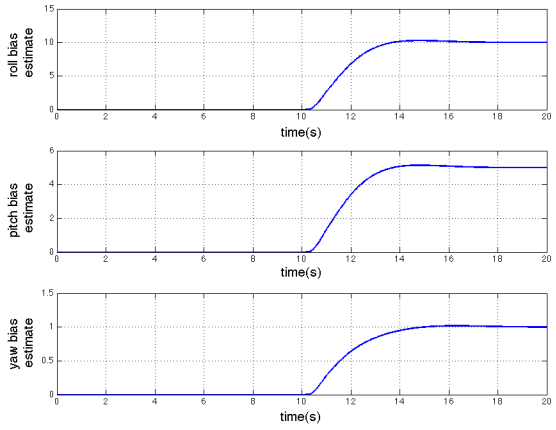

Figure 6. Estimation of gyroscope bias

6. CONCLUSION AND FUTURE WORK

In this paper, we present the design of a nonlinear fault diagnostic method for sensor bias faults in accelerometer and gyroscope measurements of quadrotor UAVs. Based on the idea that accelerometer and gyroscope measurements coincide with translational and rotational forces acting on the body, respectively, two FDI estimators are designed to generate structured residuals for fault detection and isolation. In addition, nonlinear adaptive estimation estimation schemes are presented to provide an estimate of the sensor bias. The effectiveness of the proposed method is illustrated through simulation examples.

In this paper we assumed that Euler angles are available directly for FDI design (for instance, from a motion capture camera system). In some real-world applications, this assumption may not be satisfied. Therefore, the consideration of attitude angle estimation as well as investigation of actuator faults is a direction for future research. In addition, further evaluation of the sensor bias fault diagnostic method through experimental studies with noisy measurements will be conducted.

REFERENCES

Bangura, M., & Mahony, R. (2012). Nonlinear dynamic modelling for high performance control of a quadrotor. In *Proceedings of Austrasian Conference on Robotics and Automation.*

Blanke, M., Kinnaert, M., Lunze, J., & Staroswiecki, M. (2005). *Diagnosis and Fault-Tolerant Control*. Springer.

Bramwell, A., Done, G., & Balmford, D. (2001). *Bramwell's Helicopter Dynamics*. Oxford: Butterworth-Heinemann.

Castillo, P., Lozano, R., & Dzul, A. (2005). *Modelling and Control of Mini-Flying Machines*. Springer-Verlag.

Dydek, Z. T., Annaswamy, A. M., & Lavretsky, E. (2013). Adaptive control of quadrotors uavs: A design trade study with flight evaluations. *IEEE Transaction on Automatic Control Systems Technology*, *21*(4).

Freddi, A., Longhi, S., & Monteriú, A. (2009). A model-based fault diagnosis system for a mini-quadrotor. In *7th Workshop on Advanced Control and Diagnosis.*

Guenard, N., Hamel, T., & Mahony, R. (2008). A practical visual servo control for an unmanned aerial vehicle. *IEEE Transaction on Robotics*, *24*(2).

Heredia, G., Ollero, A., Mahtani, R., & Bejar, M. (2005). Detection of sensor faults in autonomous helicopters. In *International Conference on Robotics and Automation.*

Ioannou, P. A., & Sun, J. (1996). *Robust Adaptive Control*. Dover Publications, Inc.

Ireland, M., & Anderson, D. (2012). Development of navi-

gation algorithms for NAP-of-the-earth UAV flight in a constrained urban environment. In *28th International Congress of the Aeronautical Sciences.*

Lantos, B., & Marton, L. (2011). Nonlinear Control of Vehicles and Robots. In (chap. Nonlinear Control of Airplanes and Helicopters). Springer-London.

Leishman, R. C., Jr., J. C. M., Beard, R. W., & McLain, T. (2014). Quadrotors and accelerometers. state estimation with an improved dynamic model. *IEEE Control Systems Magazine*, *34*(1).

Martin, P., & Salaün, E. (2010). The true role of accelerometer feedback in quadrotor control. In *IEEE International Conference on Robotics and Automtation.*

Pounds, P., Mahony, R., & Gresham, J. (2004). Towards dynamically-favourable quad-rotor aerial robots. In *Australasian Conference on Robotics and Automation, ACRA.*

Sharifi, F., Mirzaei, M., Gordon, B. W., & Zhang, Y. (2010). Fault tolerant control of a quadrotor UAV using sliding mode control. In *2010 Conference on Control and Fault Tolerant Systems.*

Shima, T., & Rasmussen, S. (2008). Uav cooperative decision and control: Challenges and practical approaches. In *SIAM.*

US Dept. of Defense. (2000). *Unmanned systems integrated roadmap,FY2000-2025* (Tech. Rep.). Secretary of Defense, Washington, D.C.

US Dept. of Defense. (2012). *Unmanned systems integrated roadmap FY2011-2036* (Tech. Rep.). Secretary of Defense, Washington, D.C.

Vachtsevanos, G., Tang, L., Drozeski, G., & Gutierrez, L. (2005). From mission planning to flight ocntrol of unmanned aerial vehicles: Strategies and implementation tools. *Anual Reviews in Control*, *29*, 101-115.

Zhang, X. (2011). Sensor bias fault detection and isolation in a clas of nonlinear uncertain systems using adaptive estimation. *IEEE Transaction on Automatic Control*, *56*(5).

Zhang, X., Polycarpou, M., & Parsini, T. (2001). Robust fault isolation for a class of non-linear input-output systems. *International Journal Control*, *74*(13).

BIOGRAPHIES

Remus C. Avram is a PhD candidate at Wright State Univerisity, Dayton OH. Remus, received his B.S. in Electrical Engineering with concetration in Computer Engineering at University of Texas, San Antonio, Texas in 2009. In 2011, Remus obtained his M.S. in Electrical Engineering with concetration in Control Systems from Wright Satte University, Dayton, Ohio. He is currently pursuing a doctoral degree in Electrical Engineering. Remus's main research include nonlinear health diagnostics and real-time intelligent control.

Xiaodong Zhang received the B.S. degree from Huazhong University of Science and Technology, Wuhan, China, the M.S. degree from Shanghai Jiao Tong University, Shanghai, China, and the Ph.D. degree from University of Cincinnati, Cincinnati, OH, USA, all in electrical engineering, in 1994, 1997 and 2001, respectively. He is currently an Associate Professor of Electrical Engineering Department, Wright State University, Dayton, OH. His research interests include intelligent control systems, fault diagnosis and prognosis, fault-tolerant control, verification and validation of control systems for safety assurance, etc. He is an Associate Editor of the IEEE Transactions on Control Systems Technology and a member of the IFAC SAFEPROCESS Technical Committee.

Jacob Campbell is a senior electronics engineer in the Air Force Research Laboratory, Reference Systems Branch at Wright-Patterson AFB, Ohio. He received his Ph.D. in electrical engineering from Ohio University. Currently, he manages several Air Force navigation efforts, is the technical representative for DARPAs cold atom inertial research, and serves as team lead for automated aerial refueling navigation technologies. His research interests include navigation in GPS-degraded environments.